The Journal of the Astronautical Sciences, Vol. 53, No. 2, April–June 2005, pp. 193–205

Relating Position Uncertainty to Maximum Conjunction Probability

Salvatore Alfano[1]

Abstract

The effects of positional uncertainty on the Gaussian probability computation for orbit conjunction are examined and an upper bound determined. Relative motion between two objects is assumed linear for a given encounter with time-invariant position covariance. A method is developed to assess the maximum probability for various satellite sizes, encounter geometries, and covariance sizes and shapes. The associated standard deviation then defines the boundary of probability dilution. The assertion is made that orbit positions should be sufficiently accurate to avoid this dilution region. This work shows how to calculate the upper bounds of probability by assuming worst-case covariance orientation and size. Power series approximations are developed for aspect ratios ranging from 1 to 50 to capture 99% of all conjunction possibilities. An analytical approximation is also given for an infinite aspect ratio to capture all possibilities. These expressions can be used as a simple pre-filter or to determine worst-case scenarios. Although desired, the actual covariances are not needed. What is needed is the ratio of major-to-minor axes of the projected combined covariance ellipse, the object sizes, and the relative distance at the point of closest approach.

Introduction

Probability calculations for conjunction analysis should ensure sufficient accuracy to give meaningful results. Because all operational decisions are ultimately made with respect to the amount of acceptable risk, the action threshold should not be based on an unacceptable miss distance but rather on an unacceptable collision probability. This is already done with the International Space Station and Space Transportation System where avoidance maneuvers are initiated if the collision probability exceeds an acceptable risk threshold. If the positional uncertainty is very large, a Gaussian calculation will produce a low conjunction probability. Although mathematically correct, the resulting probability may give a false sense of confidence that a conjunction is not likely to occur. Such a low probability may, in fact, indicate that the data are not of sufficient accuracy to produce an operationally meaningful result.

[1]Technical Program Manager, Center for Space Standards and Innovation, 7150 Campus Drive, Suite 260, Colorado Springs, CO 80920.

The accuracy of positional covariance matrices resulting from Least Squares Orbit Determination of sparse data is questionable. Covariance matrices formed in this manner often provide overly optimistic results. Frisbee and Foster [1] noted that "The primary problem with state error covariances determined from observations of objects in Earth orbit is that they are not truly reflective of the uncertainties in the dynamic environment." To address this concern, they devised a method to scale covariances provided to NASA by Air Force Space Command. This paper details a way to address the inaccuracy of covariance matrices by determining a mathematical upper bound that will not be exceeded regardless of satellite positional uncertainty.

Much work has been done to address the computing of collision probability for neighboring space objects [1–9] and some work has been done to examine accuracy requirements associated with those computations [10]. Typically, one determines if and when a secondary object will transgress a user-defined safety zone. The uncertainties associated with position are represented by three-dimensional Gaussian probability densities. These densities take the form of covariance matrices and can be obtained from the owner-operators or independent surveillance sources such as the US Satellite Catalog (Special Perturbations). Positions and covariances are propagated to the time of closest approach.

It is possible to find the absolute worst-possible covariance size and orientation that maximizes the probability for a given encounter where the object sizes are known and the closest-approach distance is fixed. It is also possible to find covariance parameters that maximize the probability for various covariance shapes as determined by the aspect ratio (i.e., the ratio of major-to-minor axes of the projected combined covariance ellipse). Charts were previously created to assess such probabilities [11]; this work details the mathematics used to create those charts.

If the maximum probability is below a predefined user threshold, then no further calculations are needed. Even in the absence of known covariances, the numerical approximations that follow will still provide the user with worst-case collision potential for aspect ratios ranging from 1 to 50, capturing 99% of all conjunction possibilities. Beyond those bounds, an iterative search method is recommended. Such analysis can be insightful when one only has knowledge of the miss distance and physical object sizes.

Collision Probability Computation

There are many assumptions that reduce the problem's complexity. The physical objects are treated as spheres, thus eliminating the need for attitude information (Fig. 1). Their relative motion is considered linear for the encounter by assuming the effect of relative acceleration is dwarfed by that of the velocity. The positional errors are assumed to be zero-mean, Gaussian, uncorrelated, and constant for the encounter. The relative velocity at the point of closest approach is deemed sufficiently large to ensure a brief encounter time and static covariance. The encounter region is defined when one object is within a standard deviation (σ) combined covariance ellipsoid shell scaled by a factor of n. This user-defined, three-dimensional, n-σ shell is centered on the primary object; n is typically in the range of three to eight to accommodate conjunction possibilities ranging from 97.070911% to 99.999999%.

Because the covariances are expected to be uncorrelated, they are simply summed to form one, large, combined, covariance ellipsoid that is centered at the primary object (Fig. 2). The secondary object passes quickly through this ellipsoid

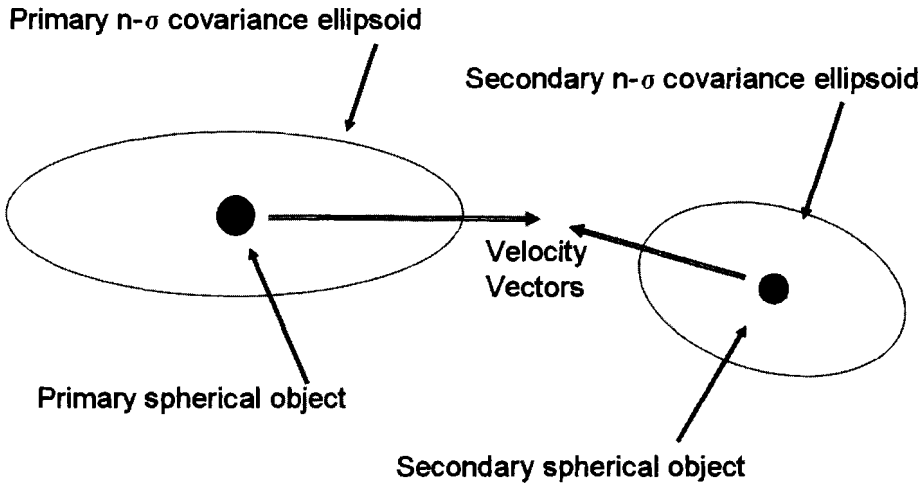

FIG. 1. Conjunction Encounter Geometry.

creating a tube-shaped path. A conjunction occurs if the secondary sphere touches the primary sphere, i.e., when the distance between the two projected object centers is less than the sum of their radii. The radius of this collision tube is enlarged to accommodate all possibilities of the secondary touching the primary by combining the radii of both objects.

A plane perpendicular to the relative velocity vector is formed and the combined object and covariance ellipsoid are projected onto this encounter plane. As stated previously, the encounter region is defined by an n-σ shell determined by the user to sufficiently account for conjunction possibilities. Within that shell the tube is

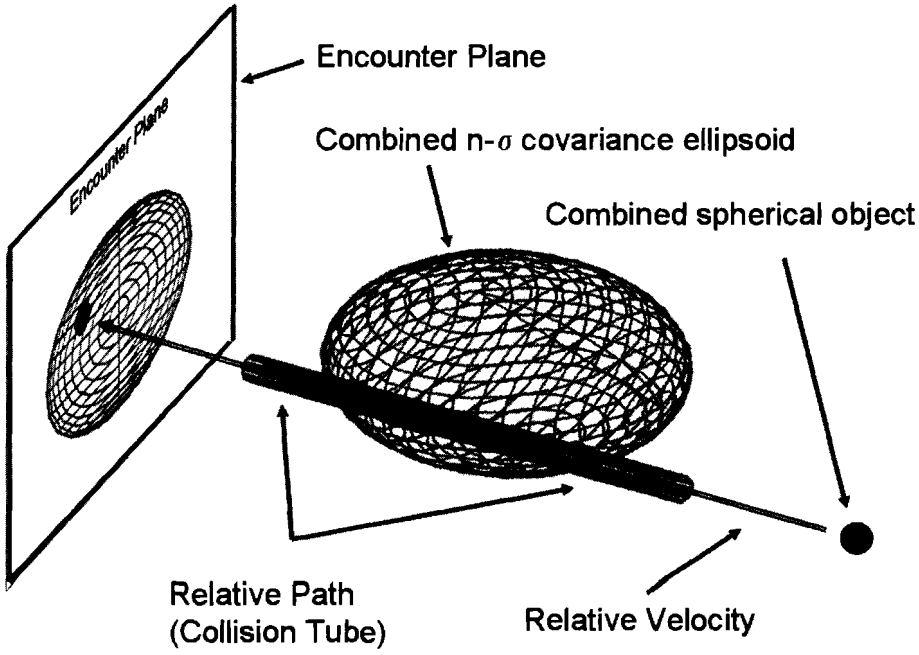

FIG. 2. Conjunction Encounter Visualization and Reduction.

straight and rapidly traversed, allowing a decoupling of the dimension associated with the tube path (i.e., relative velocity). The tube becomes a circle on the projected encounter plane. Likewise, the covariance ellipsoid becomes an ellipse (Fig. 3).

The relative velocity vector (decoupled dimension) is associated with the time of closest approach. The conjunction assessment here is concerned with cumulative probability over the time it takes to span the n-σ shell, not an instantaneous probability at a specific time within the shell. Along this dimension, integration of the probability density across the shell produces a number very near unity, meaning the close approach will occur at some time within the shell with near absolute certainty. Thus the cumulative collision probability is reduced to a two-dimensional problem in the encounter plane that is then multiplied by the decoupled dimension's probability. By rounding the latter probability to one, it is eliminated from further calculations.

The resulting two-dimensional probability equation in the encounter plane is given as

$$P = \frac{1}{2\pi\sigma x\sigma y}\int_{-OBJ}^{OBJ}\int_{-\sqrt{OBJ^2-(x)^2}}^{\sqrt{OBJ^2-(x)^2}} \exp\left[\left(\frac{-1}{2}\right)\left[\left(\frac{x+xm}{\sigma x}\right)^2+\left(\frac{y+ym}{\sigma y}\right)^2\right]\right] dy\,dx \tag{1}$$

where OBJ is the combined object radius, x lies along the minor axis, y lies along the major axis, xm and ym are the respective components of the projected miss distance, and σx and σy are the corresponding standard deviations. For the formulation that follows, the aspect ratio AR is incorporated as a multiple of the minor axis standard deviation (AR $\geq$ 1) and equation (1) is expressed as

$$P = \frac{1}{2\pi\sigma x^2 AR}\int_{-OBJ}^{OBJ}\int_{-\sqrt{OBJ^2-(x)^2}}^{\sqrt{OBJ^2-(x)^2}} \exp\left[\left(\frac{-1}{2}\right)\left[\left(\frac{x+xm}{\sigma x}\right)^2+\left(\frac{y+ym}{\sigma xAR}\right)^2\right]\right] dy\,dx \tag{2}$$

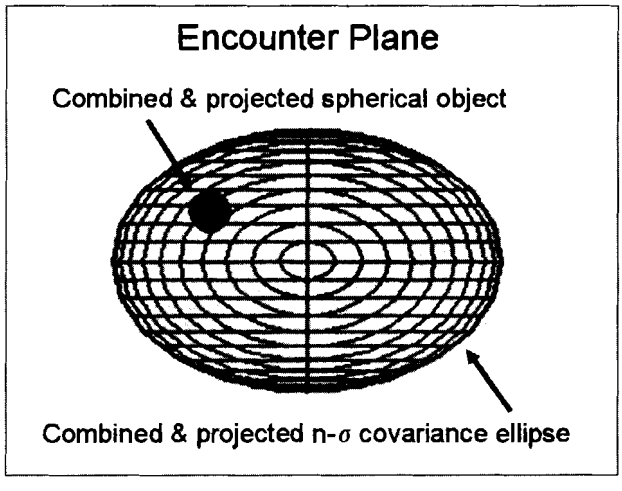

FIG. 3. Projection onto the Encounter Plane.

Maximum Probability Formulation

This formulation determines the worst-case conjunction scenario by finding the combined Gaussian probability density that maximizes collision probability. The only parameters required are distance (*dist*) of closest approach, the radius of the combined object (*OBJ*), and the ratio of major-to-minor projected covariance ellipse axes (*AR*). The major axis of the combined covariance ellipse is aligned with the relative position vector (at the point of closest approach) such that it passes through the center of the combined object. The projected, combined object is assumed circular with its probability mass distributed symmetrically about the major axis. This means that only a single axis length needs to be examined to maximize the probability, the other being determined from the aspect ratio.

Clearly, if the combined object footprint contains the covariance ellipsoid center, the minor axis' standard deviation can be chosen to drive the maximum probability to one. For spherical objects this occurs when the predicted miss distance is less than the combined object size ($dist < OBJ$). This is the limiting case and need not be addressed; it is inferred that a decision maker faced with such a predicted "direct hit" would not need a probability calculation. The method described here only applies when the combined object does not encompass the covariance center ($dist \geq OBJ$). Given the combined object radius and distance from center, the minor axis size can be determined by maximizing a two-dimensional probability expression. Once determined, the worst-case collision probability is calculated.

In the encounter plane, the *xm* and *ym* components are varied as a function of the fixed relative distance (*dist*) and the angle θ (Fig. 4).

This is the first step in determining the orientation of the distance vector with respect to the covariance axes to produce the greatest probability. Equation (2) becomes

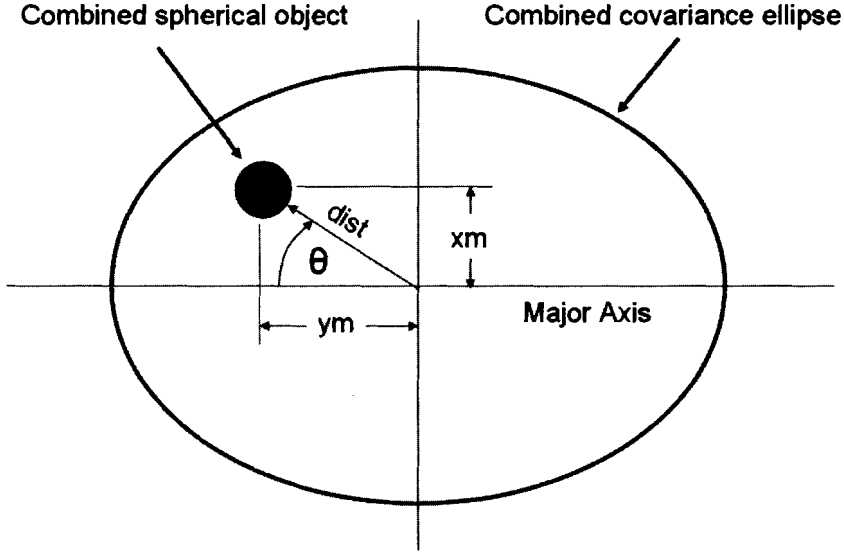

FIG. 4. Projected Position Relative to θ Angle.

$$P = \frac{1}{2\pi\sigma x^2 AR} \int_{-OBJ}^{OBJ} \int_{-\sqrt{OBJ^2-(x)^2}}^{\sqrt{OBJ^2-(x)^2}} \exp\left[\left(\frac{-1}{2}\right)\left[\left(\frac{x + dist\sin(\theta)}{\sigma x}\right)^2 + \left(\frac{y + dist\cos(\theta)}{\sigma x AR}\right)^2\right]\right] dy\,dx \quad (3)$$

The derivative with respect to θ is then set equal to zero to find the occurrences of maximum probability. The derivative equals zero whenever θ is an integer multiple of $\pi/2$. The probability is at a maximum whenever θ is an integer multiple of π. This means that the maximum probability occurs when the relative distance is along the major axis ($xm = 0, ym = dist$)

$$P = \frac{1}{2\pi\sigma x^2 AR} \int_{-OBJ}^{OBJ} \int_{-\sqrt{OBJ^2-(x)^2}}^{\sqrt{OBJ^2-(x)^2}} \exp\left[\left(\frac{-1}{2}\right)\left[\left(\frac{x}{\sigma x}\right)^2 + \left(\frac{y + dist}{\sigma x AR}\right)^2\right]\right] dy\,dx \quad (4)$$

The constant term is then brought outside the integral

$$P = \frac{\exp\left[\left(\frac{-1}{2}\right)\frac{dist^2}{\sigma x^2 AR^2}\right]}{2\pi\sigma x^2 AR} \int_{-OBJ}^{OBJ} \int_{-\sqrt{OBJ^2-(x)^2}}^{\sqrt{OBJ^2-(x)^2}} \exp\left[\left(\frac{-1}{2}\right)\left[\left(\frac{x}{\sigma x}\right)^2 + \left(\frac{y^2 + 2ydist}{\sigma x^2 AR^2}\right)\right]\right] dy\,dx \quad (5)$$

The exponential term inside the integral is expanded to various orders and the derivative of the probability equation taken with respect to σx. The resulting expression is set equal to zero to determine the minor axis standard deviation that maximizes the probability. An exact analytical solution does not exist, so a numerical search must be performed or an approximate expression used.

To assist the reader, several approximate expressions were derived for the maximum probability ($Pmax$) and its associated minor-axis standard deviation (σx). The zero-order expression for σx ($\sigma x0$) becomes

$$\sigma x0 = \frac{dist}{\sqrt{2}AR} \quad (6)$$

The first-order expression ($\sigma x1$) is

$$\sigma x1 = \sqrt{\frac{(AR^2 + 1)OBJ^2 + 2dist^2 + \sqrt{[(AR^2 + 1)OBJ^2]^2 + 4dist^4}}{8AR^2}} \quad (7)$$

The second order expression ($\sigma x2$) can be found from the expressions

$$a = 384AR^6 \quad (8)$$

$$b = -96[(1 + AR^2)OBJ^2 + 2dist^2]AR^4 \quad (9)$$

$$c = 6(OBJAR)^2[(28 + 4AR^2)dist^2 + (3 + 3AR^4 + 2AR^2)OBJ^2] \quad (10)$$

$$d = -(dist\,OBJ)^2[(2AR^2 + 3 + 3AR^4)OBJ^2 + 24dist^2] \quad (11)$$

$$0 = a(\sigma x2^2)^3 + b(\sigma x2^2)^2 + c(\sigma x2^2) + d \quad (12)$$

The third-order polynomial is solved for $\sigma x2^2$ and any complex numbers are discarded. The positive square root(s) of the remaining $\sigma x2^2$ are then tested to determine which root produces the maximum probability.

Numerical approximations to the maximum probability equation were also derived using the associated standard deviation σx_{Pmax}. The actual value of σx_{Pmax} can be set to $\sigma x0$, $\sigma x1$, or $\sigma x2$ depending upon accuracy requirements. The zero-order approximation ($Pmax0$) is

$$Pmax0 = \frac{OBJ^2}{2[AR(\sigma x_{Pmax})^2]} \exp\left[\frac{-1}{2}\left[\frac{dist}{AR(\sigma x_{Pmax})}\right]^2\right] \tag{13}$$

The first-order approximation ($Pmax1$) is

$$Pmax1 = \frac{OBJ^2}{16[AR^3(\sigma x_{Pmax})^4]} \exp\left[\frac{-1}{2}\left[\frac{dist}{AR(\sigma x_{Pmax})}\right]^2\right] [(-AR^2 - 1)OBJ^2 + 8AR^2(\sigma x_{Pmax})^2] \tag{14}$$

The second-order approximation ($Pmax2$) is

$$aa2 = 192AR^4(\sigma x_{Pmax})^4 \tag{15}$$

$$bb2 = (-24AR^4OBJ^2 - 24OBJ^2AR^2)(\sigma x_{Pmax})^2 \tag{16}$$

$$cc2 = (3AR^4 + 2AR^2 + 3)OBJ^4 + 24dist^2OBJ^2 \tag{17}$$

$$Pmax2 = \frac{OBJ^2}{384[AR^5(\sigma x_{Pmax})^6]} \exp\left[\frac{-1}{2}\left[\frac{dist}{AR(\sigma x_{Pmax})}\right]^2\right](aa2 + bb2 + cc2) \tag{18}$$

The third-order approximation ($Pmax3$) is

$$aa3 = -3072AR^6(\sigma x_{Pmax})^6 \tag{19}$$

$$bb3 = [(384AR^4 + 384AR^6)OBJ^2](\sigma x_{Pmax})^4 \tag{20}$$

$$cc3 = [(-32AR^4 - 48AR^2 - 48AR^6)OBJ^4 - 384dist^2OBJ^2AR^2](\sigma x_{Pmax})^2 \tag{21}$$

$$dd3 = (3AR^4 + 5 + 3AR^2 + 5AR^6)OBJ^6 + (96dist^2 + 32dist^2AR^2)OBJ^4 \tag{22}$$

$$Pmax3 = \frac{OBJ^2}{6144[AR^7(\sigma x_{Pmax})^8]} \exp\left[\frac{-1}{2}\left[\frac{dist}{AR(\sigma x_{Pmax})}\right]^2\right] (aa3 + bb3 + cc3 + dd3) \tag{23}$$

The fourth-order approximation ($Pmax4$) is

$$aa4 = 245760(AR\sigma x_{Pmax})^8 + [-30720OBJ^2(AR^2 + 1)](\sigma x_{Pmax}AR)^6 \tag{24}$$

$$bb4 = 1280[OBJAR^2(\sigma x_{Pmax})^2]^2[(3AR^4 + 3 + 2AR^2)OBJ^2 + 24dist^2] \tag{25}$$

$$cc4 = -80(OBJ^2AR\sigma x_{Pmax})^2[(96 + 32AR^2)dist^2 + (5AR^6 + 3AR^2 + 5 + 3AR^4)OBJ^2] \tag{26}$$

$$dd4 = (35AR^8 + 35 + 20AR^6 + 18AR^4 + 20AR^2)OBJ^8 + [(1200 + 480AR^2 + 240AR^4)dist^2]OBJ^6 + 1280dist^4OBJ^4 \tag{27}$$

$$Pmax4 = \frac{1}{491520[AR^9(\sigma x_{Pmax})^{10}]} \exp\left[\frac{-1}{2}\left[\frac{dist}{AR(\sigma x_{Pmax})}\right]^2\right] OBJ^2(aa4 + bb4 + cc4 + dd4) \tag{28}$$

A case of interest involves an infinite aspect ratio ($AR = \infty$). For this case, the combined object radius is normalized with respect to the miss distance

$$r = \frac{OBJ}{dist} \tag{29}$$

The covariance ellipsoid is constructed such that the combined object contains all the probability mass associated with the minor axes. The probability P for the remaining axis is reduced to

$$P = \frac{1}{\sqrt{2\pi}\sigma_u} \int_{1-r}^{1+r} \exp\left[\frac{-1}{2}\frac{u^2}{(\sigma_u)^2}\right] du \tag{30}$$

where σ_u is the normalized standard deviation. Equation (30) can be expressed in an alternate form using error functions as

$$P = \frac{1}{2}\operatorname{erf}\left[\frac{1}{2}(1 + r)\frac{\sqrt{2}}{\sigma_u}\right] + \frac{1}{2}\operatorname{erf}\left[\frac{1}{2}(-1 + r)\frac{\sqrt{2}}{\sigma_u}\right] \tag{31}$$

Probability is maximized by

$$\frac{dP}{d\sigma_u} = 0 \tag{32}$$

The result is a very simple expression for σ_u in terms of r

$$\sigma_u = \sqrt{\frac{2r}{\ln\left[\frac{(1 + r)}{(1 - r)}\right]}} \tag{33}$$

Substitution of equation (33) into (31) produces the algebraic expression

$$Pmax = \frac{1}{2}\left[\operatorname{erf}\left[\frac{(r + 1)}{2\sqrt{r}}\sqrt{-\ln\left[\frac{(1 - r)}{(1 + r)}\right]}\right] + \operatorname{erf}\left[\frac{(r - 1)}{2\sqrt{r}}\sqrt{-\ln\left[\frac{(1 - r)}{(1 + r)}\right]}\right]\right] \tag{34}$$

The length of the single axis has been optimized to produce the greatest overall probability. The reader is reminded that σ_u is a normalized value and should be multiplied by *dist* to produce σx.

Due to the near-linear nature of the previous equation, *Pmax* can be approximated to at least three significant figures with the equations

$$Pmax = 0.48394(r) \qquad (r < 0.8) \tag{35}$$

$$Pmax = 0.21329 \exp(1.01511r) - 0.09025 \qquad (0.8 \leq r < 1.0) \tag{36}$$

For the limiting case where $r = 1$, *Pmax* is 0.5. Equation (35) or (36) can easily be employed for computational prescreening.

As the aspect ratio grows, so does *Pmax*. To properly assess the maximum probability, it is recommended that the reader not use equation (35) or (36) for anything other than prescreening unless it is certain that the encounter's aspect ratio is near infinity ($AR > 1000$).

Region of Probability Dilution

For fixed object sizes and miss distance, the σx that produces *Pmax* defines the dilution region boundary as shown in Fig. 5. To left of the vertical line, greater positional accuracy (smaller σx) decreases collision probability. To the right of the vertical line, lesser positional accuracy (greater σx) also decreases collision probability. Both good and poor quality data can produce the same probability (10^{-6} is given as an example in Fig. 5). Although both calculations are mathematically correct, only the former is operationally meaningful.

The probability dilution region is that region where the standard deviation of the combined covariance minor axis (σx) exceeds that which yields *Pmax*. If operating outside this dilution region (left of vertical line) it is reasonable to associate low probability with low risk. If operating within the dilution region, then the farther into this region the uncertainty progresses the more unreasonable it becomes to associate low probability with low risk. If the positional uncertainty is large enough, the resulting low probability may mislead the user into thinking the encounter poses little or no threat. Therefore, a low probability in the dilution region may be the result of poor quality data and should be treated accordingly.

The dilution region boundary should be used to determine the minimum accuracy requirement for a meaningful probability assessment. When calculating true probability from equation (1), the reader is advised to always consider this region. If the positional data are not of sufficient quality to avoid this region, then obtain better (more accurate) data and reassess the true probability. If better data are not available or still insufficient, consider using the maximum probability as opposed to the true one. This will ensure that a decision maker is not lulled into a false sense of security by a low probability calculation that is specious.

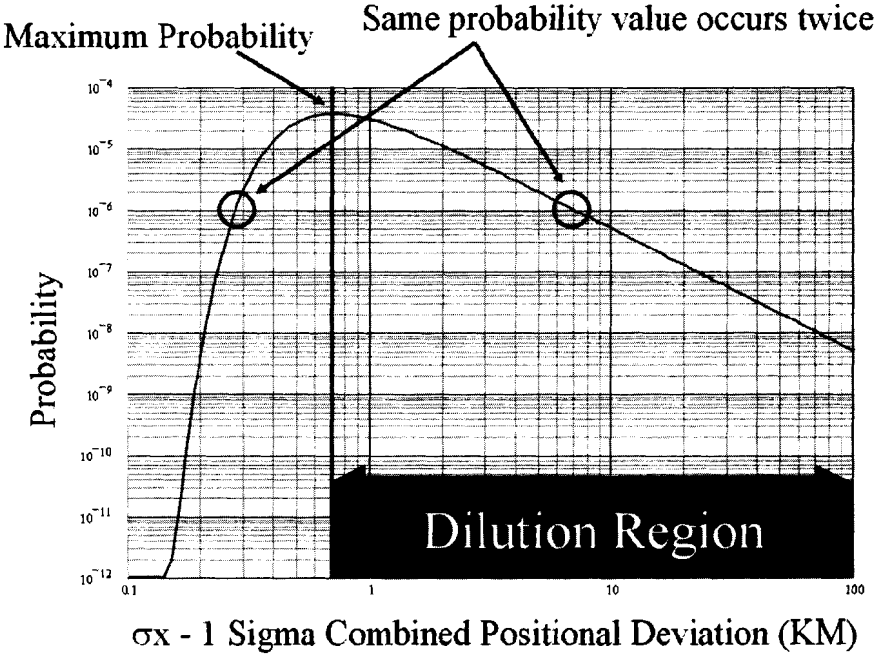

FIG. 5. Dilution Region Defined for Notional Encounter.

Numerical Testing

The σx and $Pmax$ equations are approximations, making it necessary to test their accuracy limits. Testing was done by varying the combined object radii from 1 to 100 meters ($1 \leq OBJ \leq 100$), the aspect ratios from 1 to 50 ($1 \leq AR \leq 50$), and relative distances from 50 meters to 10 kilometers, for all derived combinations of σx and $Pmax$. The results of numerical testing are in Table 1 for exact maximum probabilities less than 0.01 and less than 0.001. From this table, the reader can choose an approximation suitable for desired operations. If more accuracy is required then a numerical search should be performed to find the value of σx that maximizes equation (5).

Typically, a user requires no more than 99% accuracy (two significant figures) to make a collision mitigation decision. Therefore, the least computationally intensive approximation that is good to within one percent should be chosen. For a probability decision threshold less than 0.01 the $Pmax2(\sigma x1)$ expression is recommended. $Pmax1(\sigma x0)$ should be used for a decision threshold less than 0.001. Outside the described testing bounds, the user should iteratively determine the σx that maximizes equation (5) or, if warranted, assume an infinite aspect ratio and use the appropriate equation.

Choosing an Aspect Ratio

If the combined covariance is unknown, the user must decide what aspect ratio is reasonable for analysis. If equal uncertainty is assumed for all axes, then the aspect ratio will be one. For the absolute worst case imaginable the aspect ratio should be set to infinity and equation (34) or its approximation used to determine the maximum probability.

It is instructional to get a sense of the aspect ratio's variability. Every day that new NORAD two-line element sets are publicly released, a maximum conjunction

TABLE 1. Maximum Percent Error of Derived Approximations

	$Pmax < 0.01$	$Pmax < 0.001$
$Pmax0(\sigma x0)$	35.00	3.50000
$Pmax1(\sigma x0)$	18.00	0.15000
$Pmax2(\sigma x0)$	2.00	0.05000
$Pmax3(\sigma x0)$	4.70	0.05000
$Pmax4(\sigma x0)$	2.90	0.05000
$Pmax0(\sigma x1)$	24.00	3.00000
$Pmax1(\sigma x1)$	8.00	0.13000
$Pmax2(\sigma x1)$	0.31	0.00250
$Pmax3(\sigma x1)$	1.60	0.00040
$Pmax4(\sigma x1)$	1.20	0.00032
$Pmax0(\sigma x2)$	33.00	3.00000
$Pmax1(\sigma x2)$	12.00	0.13000
$Pmax2(\sigma x2)$	2.90	0.00250
$Pmax3(\sigma x2)$	1.30	0.00006
$Pmax4(\sigma x2)$	0.32	0.00005

probability report is generated and posted as a free advisory service at the website http://celestrak.com/SOCRATES/ [12]. The June 29, 2004, data were used to determine all object pairings of primaries (2,627) with secondaries (8,411) within 10 kilometers for a seven-day span. This data was coupled with time-varying covariances produced by The Aerospace Corporation's COVGEN tool [13]. The combined aspect ratio for each of the resulting 26,752 pairs was then used to produce figures that show variability.

The reader is advised that the covariances used to produce the figures are not statistically formal due to the nature of COVGEN processing [13]. The estimates of error and error growth for each object are obtained by processing a time history of SGP4 element sets for each object while assuming zero bias. The differences in the Radial, Transverse, and Normal components are then found and quadratic estimation determines their error growth. This method can underestimate the initial error at epoch, so a separate method is used to determine such. If one is willing to consider COVGEN results as sufficiently proper representations of the positional covariances then Figs. 6 and 7 can be used to choose an acceptable bound for the aspect ratio.

Figures 6 and 7 are representative of day-to-day occurrences. As seen in Fig. 7, 99% of all conjunctions have an aspect ratio of 40 or less. 99.9% of all conjunctions have an aspect ratio of 70 or less (not shown). The maximum aspect ratio rarely exceeds 140.

It is obviously desirable to use the most representative covariances possible, thus ensuring the correct aspect ratio for each and every conjunction. As previously stated, a larger aspect ratio will result in a larger value for *Pmax*. Using a default aspect ratio of 40 or 70, sufficient to capture most conjunctions, will cause the maximum probability to be overinflated for many of those conjunctions. Although not ideal, this may be the best assessment possible if the covariance data are insufficient or not available.

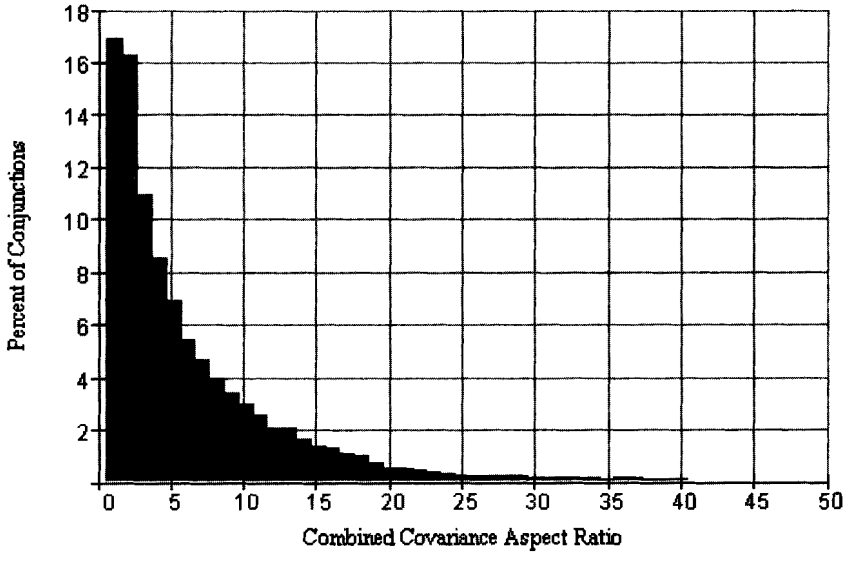

FIG. 6. Aspect Ratio Histogram.

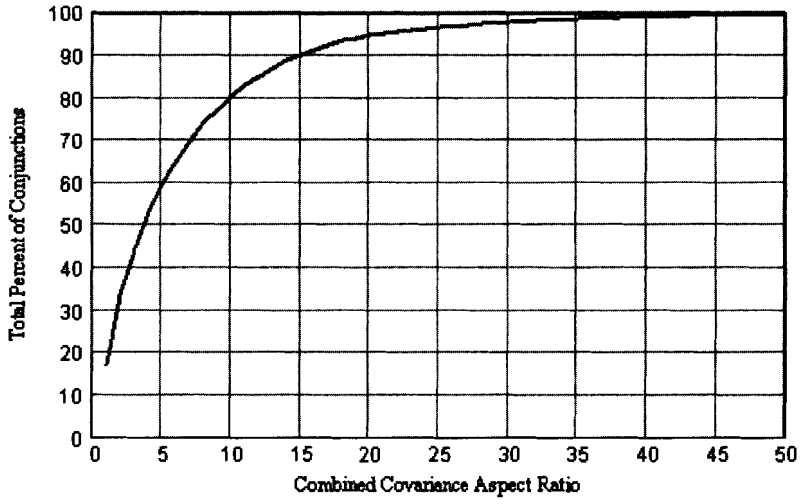

FIG. 7. Cumulative Percentage Versus Aspect Ratio.

Conclusion

Formulations for maximum probability and its associated standard deviation were derived and then approximated using truncated power series. The approach assumes that the major axis of the combined covariance ellipse passes through the center of the combined object thereby maximizing the probability for any aspect ratio. Given the radius of the combined object and its distance from covariance center, the size of the minor axis is determined by maximizing a two-dimensional probability expression. Once determined, the worst-case collision probability can be calculated. Expressions were shown sufficient to at least two significant figures for aspect ratios ranging from 1 to 50, thus capturing over 99% of all conjunction possibilities. The analytical approximation for an infinite aspect ratio captures all possibilities. Using an all-encompassing aspect ratio (as opposed to the exact one) may cause the maximum probability to be overinflated. Although not ideal, this may be the best assessment possible if the covariance data are insufficient or not available.

The region of probability dilution was also defined. In this region low probability does not necessarily indicate low risk. A large positional uncertainty can yield a low probability which may mislead the user into thinking the encounter poses little or no threat. If in this region, it is recommended that the user obtain better (more accurate) data and reassess the probability. If this cannot be done, decisions should be based on the maximum probability as opposed to the true probability.

To compute the maximum probability, the only parameters required are the distance between the objects at the point of closest approach, the radius of the combined object, and the assumed ratio of the projected major and minor combined covariance ellipse axes. Such analysis can be helpful when one lacks knowledge of positional uncertainties or to address hypothetical scenarios. Several options were presented for choosing an aspect ratio in the complete absence of covariance information.

References

[1] FOSTER, J. L. and ESTES, H. S. "A Parametric Analysis of Orbital Debris Collision Probability and Maneuver Rate for Space Vehicles," NASA JSC 25898, August 1992.

[2] KHUTOROVSKY, Z. N., BOIKOV, V., and KAMENSKY, S. Y. "Direct Method for the Analysis of Collision Probability of Artificial Space Objects in LEO: Techniques, Results, and Applications," *Proceedings of the First European Conference on Space Debris,* ESA SD-01, 1993, pp. 491–508.

[3] CARLTON-WIPPERN, K. C. "Analysis of Satellite Collision Probabilities Due to Trajectory and Uncertainties in the Position/Momentum Vectors," *Journal of Space Power,* Vol. 12, No. 4, 1993.

[4] CHAN, K. F. "Collision Probability Analyses for Earth Orbiting Satellites," *Advances in the Astronautical Sciences,* Vol. 96, 1997, pp. 1033–1048.

[5] BEREND, N. "Estimation of the Probability of Collision Between Two Catalogued Orbiting Objects," *Advances in Space Research,* Vol. 23, No. 1, 1999, pp. 243–247.

[6] OLTROGGE, D. and GIST, R. "Collision Vision Situational Awareness for Safe and Reliable Space Operations," 50th International Astronautical Congress, October 4–8, 1999, Amsterdam, The Netherlands, IAA-99-IAA.6.6.07.

[7] AKELLA, M. R. and ALFRIEND, K. T. "Probability of Collision Between Space Objects," *Journal of Guidance, Control, and Dynamics,* Vol. 23, No. 5, September-October 2000, pp. 769–772.

[8] CHAN, K. F. "Analytical Expressions for Computing Spacecraft Collision Probabilities," presented as paper AAS 01-119 at the AAS/AIAA Space Flight Mechanics Meeting, Santa Barbara, California, February 11–15, 2001.

[9] PATERA, R. P. "General Method for Calculating Satellite Collision Probability," *AIAA Journal of Guidance, Control, and Dynamics,* Volume 24, Number 4, July-August 2001, pp. 716–722.

[10] GOTTLIEB, R. G., SPONAUGLE, S. J., and GAYLOR, D. E. "Orbit Determination Accuracy Requirements for Collision Avoidance," presented as paper AAS 01-181 at the AAS/AIAA Space Flight Mechanics Meeting, February 11–15, 2001, Santa Barbara, California.

[11] ALFANO, S. "Relating Position Uncertainty to Maximum Conjunction Probability," presented as paper AAS 03-548 at the AAS/AIAA Astrodynamics Specialist Conference, August 3–7, 2003, Big Sky, Montana.

[12] KELSO, T. S. and ALFANO, S. "Satellite Orbital Conjunction Reports Assessing Threatening Encounters in Space (SOCRATES)," presented as paper AAS 05-124 at the AAS/AIAA Space Flight Mechanics Meeting, January 23–27, 2005, Copper Mountain, Colorado.

[13] PETERSON, G. E., GIST, R. G., and OLTROGGE, D. L. "Covariance Generation for Space Objects using Public Data," presented as paper AAS 01-113 at the AAS/AIAA Space Flight Mechanics Meeting, February 11–15, 2001, Santa Barbara, California.